

conjugation and crystal forces in determining the preferred molecular geometry.

The (90°,90°) conformation lies 25.3 kJ·mol<sup>-1</sup> above the minimum according to the STO-3G results. As mentioned previously,<sup>32</sup> this value is comparable to the barrier to internal rotation in benzaldehyde, which lies in the range 19.3–22.7 kJ·mol<sup>-1</sup> for various experimental methods<sup>37–40</sup> and 24 kJ·mol<sup>-1</sup> from an STO-3G calculation.<sup>34,35</sup> In both molecules, the origin of the barrier is presumably the loss of  $\pi$ -conjugation between the phenyl and keto groups. It is perhaps surprising therefore that the loss of conjugation between the keto group and one phenyl group in benzaldehyde should require as much energy as the loss of conjugation between the keto group and both phenyl groups in benzophenone. From the 3-21G//STO-3G results, the barrier is 57.2 kJ·mol<sup>-1</sup>.

Although the more flexible split-valence basis provides a lower total energy, it leads to larger relative energies than the STO-3G basis. The 3-21G barrier heights are roughly twice the STO-3G values. Because the STO-3G barrier for benzaldehyde is in better agreement with experiment<sup>37–40</sup> than the estimates obtained from 4-21G, 4-31G, or 6-31G split-valence bases,<sup>35</sup> this is not unexpected. Presumably, this agreement is a result of a fortuitous cancellation of errors at the STO-3G level, perhaps associated with the compactness of the STO-3G basis functions.

**Torsional Frequencies.** Lines in the T<sub>1</sub> ← S<sub>0</sub> absorption spectrum have been tentatively assigned to torsional modes of the triplet state at 85 and 100 cm<sup>-1</sup>, which would correspond to B and A modes, respectively, in C<sub>2</sub> symmetry.<sup>33</sup> Progressions in the <sup>1</sup>n $\pi^*$  ← S<sub>0</sub> spectrum were assigned to the same A mode at 80 cm<sup>-1</sup> because the B mode cannot form progressions. From semi-empirical and ab initio calculations of the harmonic vibrational frequencies of the C<sub>2</sub> minimum energy conformer, the torsional frequency corresponding to the minimum energy path (B mode)

is 23 cm<sup>-1</sup> from AM1 or 32 cm<sup>-1</sup> from STO-3G. Torsion along the  $\psi_2 = \psi_1$  diagonal (A mode) appears at 56 cm<sup>-1</sup> according to AM1, or 57 cm<sup>-1</sup> according to the STO-3G calculation. Although the calculated normal coordinates corresponding to these frequencies may be inaccurate, a harmonic approximation to the AM1 surface in the vicinity of the minimum supports these assignments. The third-lowest and fourth-lowest calculated vibrational frequencies are 85 and 133 cm<sup>-1</sup> from AM1, or 97 and 152 cm<sup>-1</sup> from STO-3G. According to the normal coordinate descriptions, these are skeletal modes of A and B symmetry, respectively, and not the torsions. Possibly, the observed vibrations<sup>33</sup> of the excited singlet and triplet correspond to these skeletal modes. Experimental investigation of these low-frequency motions would be helpful.

### Conclusions

On the basis of AM1 and STO-3G calculations, the preferred conformation of benzophenone has C<sub>2</sub> symmetry. The angle between the planes defined by a phenyl ring and the keto group is about 33°, and the angle between the phenyl ring planes is about 56°. These results are in excellent agreement with crystallographic data. The barrier to internal rotation in benzophenone is probably between 3.0 and 5.6 kJ·mol<sup>-1</sup>. The minimum energy path for conformational interconversion is determined by a balance between the maintenance of  $\pi$ -conjugation between the keto group and the phenyl rings and the avoidance of mutual repulsion of the phenyl rings. These findings are in agreement with early results from extended Hückel theory. With the 3-21G basis and the STO-3G optimum geometry, the rotational barrier is 12.0 kJ·mol<sup>-1</sup>, which is probably an overestimate. From the AM1 and STO-3G results, the torsional frequency corresponding to the antisymmetric mode is estimated to be 23 and 32 cm<sup>-1</sup>, respectively, and the torsional frequency corresponding to the symmetric mode is estimated to be 56 and 57 cm<sup>-1</sup>, respectively. An experimental determination of the torsional frequencies would be valuable.

**Acknowledgment.** This work was supported by a grant to T.A.W. from the Natural Sciences and Engineering Research Council of Canada. Some of the ab initio calculations were performed on the Cray-XMP/24 supercomputer at the Ontario Center for Large-Scale Computation.

- (37) Miller, F. A.; Fateley, W. G.; Witkowski, R. E. *Spectrochim. Acta A* 1967, 23, 891.  
 (38) Kakar, R. K.; Rinehart, E. A.; Quade, C. R.; Kojima, T. *J. Chem. Phys.* 1970, 52, 3803.  
 (39) Glebova, L. A.; Pentin, Yu. A.; Tyulin, V. I. *Vestn. Mosk. Univ., Khim., Ser. 2* 1980, 21.  
 (40) Durig, J. R.; Bist, H. D.; Furic, K.; Qui, J.; Little, T. S. *J. Mol. Struct.* 1985, 129, 45.

## Implementation of Nonadditive Intermolecular Potentials by Use of Molecular Dynamics: Development of a Water–Water Potential and Water–Ion Cluster Interactions

James Caldwell,<sup>†</sup> Liem X. Dang,<sup>†</sup> and Peter A. Kollman<sup>\*,†</sup>

Contribution from the Department of Pharmaceutical Chemistry, School of Pharmacy, University of California, San Francisco, California 94143, and IBM Research Division, Almaden Research Center, 650 Harry Road, San Jose, California 95120-6099. Received March 12, 1990

**Abstract:** We present the results of simulations using water–water and water–ion models that include explicit nonadditive polarization energies. The water–water potential has been adjusted to fit the experimental water density and potential energy. The resulting potential is used in a simulation of liquid water. In addition to the density and potential energy, the model also fits the experimental radial-distribution functions and the diffusion coefficient well. Water–ion parameters are derived similarly and include, in addition to polarization nonadditivity, three-body exchange repulsion. The model is then used to compute the energy of ion–water clusters. The agreement with experimental energies of cluster formation is very good.

### Introduction

The structure and properties of liquid water are critical to our existence, as well as being representative of an important polar liquid. Thus, understanding these structures and properties from

a physical–chemical point of view has inspired a very large number of statistical mechanical models as well as computer simulation approaches. The goal of the latter is, beginning with the intra- and intermolecular energies of a water molecule as a function of coordinate, to use Monte Carlo or molecular dynamics methods to derive observable structural, kinetic, and thermodynamic properties that are consistent with experiment.

<sup>\*</sup> University of California.

<sup>†</sup> Almaden Research Center.

These energy functions fall into two broad classes: pairwise additive and "effective" two-body interaction functions. Energy functions that are pairwise additive (two-body potentials) are most reasonably derivable from quantum mechanical calculations, and the efforts of Clementi and co-workers<sup>1</sup> are the major recent effort in this direction. Far more common are "effective" two-body functions, which derive the parameters of the function by requiring a fit to a number of properties of the liquid. The classic work by Rahman and Stillinger<sup>2</sup> describes the first application of such a potential to water using molecular dynamics, and the potentials SPC/SPC/E<sup>3</sup> and TIP3P/TIP4P<sup>4</sup> are refined versions of this approach.

The key assumption in "effective" two-body potentials is that many-body interaction energies can be incorporated into the parameters that are evaluated as two-body interaction energies. This had led to partial charges on the oxygen and hydrogens that correspond to a dipole moment of the water molecule of  $\sim 2.3$ – $2.4$  D, considerably enhanced over the gas-phase value of 1.85 D.

A recent paper by Jorgensen et al.<sup>4</sup> has reviewed the simulation results with use of such potentials. These potentials appear very powerful in representing the enthalpy, density, heat capacity, radial-distribution functions, and diffusion coefficients of liquid water. Recent enhancements of such potentials have considered many-body effects in liquid water in a mean-field approximation.<sup>5</sup> These have led to further improvements and refinements in such potentials, and the SPC/E model appears to be the best available to date of this sort.<sup>3</sup>

Why have so few water models included nonadditive effects explicitly? First, such an inclusion requires a considerable increase in computation, of the order of 2–10 times. Second, the success of "effective two-body" models has dampened the enthusiasm for spending the increased computational resources required for such models. Nonetheless, until we have a successful and useful approach to describe such nonadditive models, we cannot fully assess their nature. In particular, such models are expected to be particularly important for ionic solutions, where water molecules near the ion should be significantly more polarized than those further away.

The first computer simulation on liquid water with use of explicit nonadditive models was by Barnes et al.<sup>6</sup> More recently, studies on such models by Ahlstrom et al.,<sup>7</sup> Sprik and Klein,<sup>8</sup> Cieplak et al.,<sup>9</sup> and Niesar et al.<sup>1</sup> have been informative, but to date, no one has developed a nonadditive model that has been shown to reproduce the liquid structure, density, and energy as well as effective two-body potentials. This paper presents the results of molecular dynamics simulations on a nonadditive model that succeeds in doing so. Furthermore, calculations are presented on ion-water clusters that suggest that this model has much to offer in studies of ionic solutions.

## Method

We use the following equations to describe the interaction energy of the system, which uses a rigid three-point-charges water model with the internal geometry of  $109.5^\circ$  and  $1 \text{ \AA}$  for the HOH angle and OH distance, respectively. It consists of the Lennard-Jones and electrostatic

interactions between waters and waters-ion, a nonadditive polarization energy, and a term that includes explicit exchange-repulsion nonadditivity for ion-two water interactions. Thus, the total potential is given as

$$U_{\text{tot}} = U_{\text{pair}} + U_{\text{pol}} + U_{3\text{-body}} \quad (1)$$

where the pair additive potential is

$$U_{\text{pair}} = \sum_i \sum_j A_{ij}/r_{ij}^{12} - C_{ij}/r_{ij}^6 + q_i q_j / r_{ij} \quad (2)$$

and the polarization energy is

$$U_{\text{pol}} = -1/2 \sum_i \mu_i E_i^0 \quad (3)$$

finally, the three-body potential is written as follows

$$U_{3\text{-body}} = A \exp(-\beta r_{12}) \exp(-\beta r_{13}) \exp(-\gamma r_{23}) \quad (4)$$

Here,  $\mu_i$  is the induced dipole moment and  $E_i$  is the electric field at atom  $i$

$$\mu_i = \alpha_i E_i \quad E_i = E_i^0 + \sum_{j=1, j \neq i} T_{ij} \mu_j \quad (5)$$

and  $E_i^0$  and  $T_{ij}$  are the electrostatic fields from the charges and the dipole tensor, respectively

$$E_i^0 = \sum_{j=1, j \neq i} q_j \frac{r_{ij}}{r_{ij}^3} \quad T_{ij} = \frac{1}{r_{ij}^3} \left( 3r_{ij} \frac{r_{ij}}{r_{ij}^2} - 1 \right) \quad (6)$$

where  $\alpha_i$  is the polarizability of atom  $i$ ,  $r_{ij}$  is the vector from atom  $j$  to atom  $i$ ,  $q_j$  is the charge at atom  $j$ ,  $r_{12}$  and  $r_{13}$  are ion-oxygen distances for the ion-water trimer,  $r_{23}$  is the oxygen-oxygen distance for the two water molecules involved in the ion-water trimer, and  $A$ ,  $\beta$ , and  $\gamma$  are empirical parameters.

The analytical derivative of the three-body potential is calculated with use of the chain rule, and the analytical derivative of the polarization energy, including the dipole-monopole and dipole-dipole forces, is an extension of the work of Vesely on a system of dipolar molecules<sup>11</sup> and is the same as that used in ref 7. We used the traditional iterative approach to solve eq 5 with the iteration continuing until the root mean square of the difference in the induced dipole between successive iterations is less than 0.01 D/atom. We find that self-consistency is usually achieved within five iterative steps. The atomic polarizabilities for the hydrogen and oxygen and for the ions are taken from the work of Applequist et al.<sup>12</sup> and of Sangster and Atwood,<sup>12</sup> respectively.

In constructing the nonadditive potential model, we used SPC/E water as a reference. This SPC/E model<sup>3</sup> is a reparameterized version of the SPC model to implicitly include the polarization energy. We have carried out three molecular dynamics simulations on liquid water: the first has used the SPC/E water model; the second has used a gas-phase-water dipole moment of 1.85 D and the molecular polarizability centered on the oxygen atom (POL); and the third allowed the partial charges to vary to best reproduce the properties of liquid water and used the atomic polarizabilities of Applequist<sup>12</sup> on the oxygen and the hydrogen atoms (POL1). While the structural properties of both POL and POL1 models are very similar, we find the thermodynamic properties of the model POL1 much better than the POL model. For example, the induced dipole and the potential energy/water molecule of model POL are  $1.4 \pm 0.2$  D and  $-11.5 \pm 0.1$  kcal/mol, while the model POL1 gave  $0.50 \pm 0.05$  D and  $-9.82 \pm 0.10$  kcal/mol, respectively. Since the experimental value for the water energy is  $-9.92$  kcal/mol and the induced dipole is near 0.6–0.8 D, it is clear that POL1 is a much better model and we carried out more extensive simulations with it.

The molecular dynamics simulation system consisted of 216 waters in a cubic cell (of 18.6 Å). An initial set of velocities was selected from a Maxwell-Boltzmann distribution corresponding to 300 K. Coupling constants of 0.2 and 0.5 ps for temperature and pressure were used, and the SHAKE<sup>13</sup> procedure was employed to constrain all the bond lengths to their equilibrium values. The simulation was run with a time step of 1 fs, and the nonbonded interactions were truncated at a molecule separation of 8 Å. Each simulation consisted of 20-ps equilibration followed by 40 ps of data collection. The diffusion coefficient was calculated as in ref 4, and the methodology was validated by reproducing the results

(1) Matsuoka, O.; Clementi, E.; Yoshimine, M. *J. Chem. Phys.* **1976**, *64*, 1351. Niesar, U.; Corongiu, G.; Huang, M.-J.; Dupuis, M.; Clementi, E. *Int. J. Quantum Chem., Quantum Chem. Symp.* **1989**, *23*, 421. *Modern Techniques in Computational Chemistry: MOTEC-89*; Clementi, E., Ed.; ESCOM, 1989.

(2) Rahman, A.; Stillinger, F. H. *J. Chem. Phys.* **1971**, *55*, 3336.

(3) Berendsen, H. J. C.; Grigera, J. R.; Straatsma, T. P. *J. Phys. Chem.* **1987**, *91*, 6269.

(4) Jorgensen, W. L.; Chandrasekhar, J.; Madura, J. D.; Impey, R. W.; Klein, M. L. *J. Chem. Phys.* **1983**, *79*, 926.

(5) Watanabe, K.; Klein, M. L. *J. Chem. Phys.* **1989**, *131*, 157.

(6) Barnes, P.; Finney, J. L.; Nicholas, J. D.; Quinn, J. E. *Nature* **1979**, *282*, 459.

(7) Ahlstrom, P.; Wallquist, A.; Engstrom, S.; Jonsson, B. *Mol. Phys.* **1989**, *68*, 563.

(8) Sprik, M.; Klein, M. L. *J. Chem. Phys.* **1988**, *89*, 7556.

(9) Cieplak, P.; Lybrand, T.; Kollman, P. A. *J. Chem. Phys.* **1990**, *92*, 6755.

(10) Lybrand, T. P.; Kollman, P. A. *J. Chem. Phys.* **1985**, *83*, 2923. Cieplak, P.; Lybrand, T.; Kollman, P. A. *J. Chem. Phys.* **1987**, *87*, 6393.

(11) Vesely, F. J. *J. Comput. Phys.* **1977**, *24*, 361.

(12) Applequist, J.; Carl, J. R.; Fung, K.-K. *J. Am. Chem. Soc.* **1972**, *94*, 1972. Sangster, M. J. L.; Atwood, R. M. *J. Phys. C* **1987**, *11*, 1541.

(13) Berendsen, H. J. C.; Postma, J. P. M.; Di Nola, A.; Van Gunsteren, W. F.; Haak, J. R. *J. Chem. Phys.* **1984**, *81*, 3684. Ryckaert, J. P.; Cicciotti, G.; Berendsen, H. J. C. *J. Comput. Chem.* **1987**, *1*, 266.

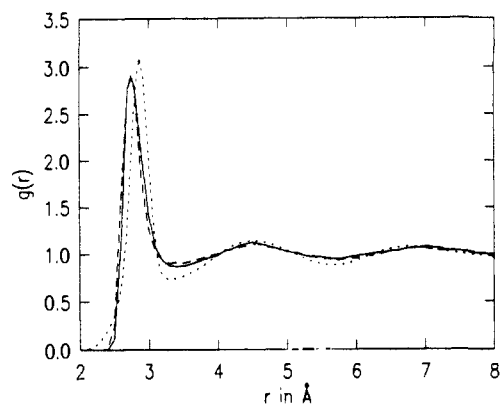


Figure 1. Oxygen-oxygen radial distribution functions: solid is the SPC/E model, dotted is X-ray,<sup>15</sup> and dashed is this work (POL1).

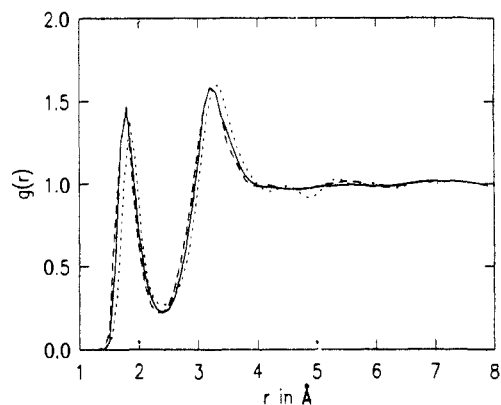


Figure 2. Same as Figure 1 for hydrogen-oxygen.

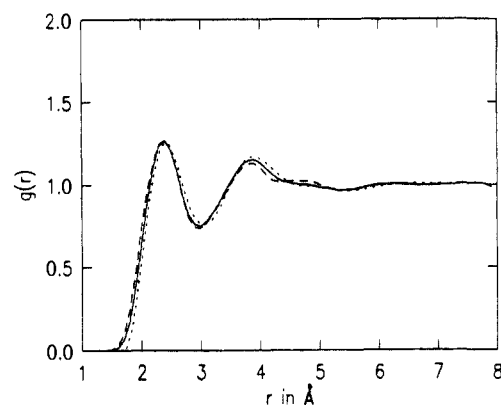


Figure 3. Same as Figure 1 for hydrogen-hydrogen.

in ref 3 on SPC/E water. Our simulations used a modified version of AMBER 3.0.<sup>14</sup> The parameters for these simulations are given in Table I.

## Results

We present the results of our molecular dynamics simulations on the new model of liquid water in Table I. Agreement with the experimental energy and density of the liquid is excellent and the agreement with the experimental radial distribution functions (Figures 1-3), diffusion coefficient, and water-dimer properties good.

The calculated oxygen-oxygen radial distribution function (RDF) of this model is very similar to the corresponding RDF of the SPC/E model (Figure 1).<sup>3</sup> The first peak of each occurs

Table I. Molecular Dynamics Simulations Results for Various Water Models<sup>a</sup>

	SPC/E	POL1 (this model)	expt <sup>h</sup>
$\sigma^b/\text{Å}$	3.160	3.160	
$\epsilon^b/\text{kcal mol}^{-1}$	0.1554	0.1554	
$q_H/e^b$	0.4238	0.3650	
$q_O/e^b$	-0.8476	-0.730	
$T/K^b$	300	303	
$P/\text{atm}^b$	1.0	1.0	
$U_{\text{tot}}^c/\text{kcal mol}^{-1}$	-9.90	$-9.82 \pm 0.10$	-9.92
$U_{\text{pol}}^c/\text{kcal mol}^{-1}$		-2.48	
$\rho^d/\text{g cm}^{-3}$	0.998	0.991 <sup>d</sup>	0.995 (305 K)
dimer $U^e/\text{kcal mol}^{-1}$		$5.5 (2.8 \text{ Å})^e$	$5.4 \pm 0.7 (2.94 \pm 0.04)$
$\mu_{\text{perm}}^f$	2.35	2.025	1.85 (gas phase)
$\mu_{\text{tot}}^f$	2.35	2.516	$\sim 2.5$
$\mu_{\text{induced}}^f$		0.507	
$\alpha_H^g/\text{Å}^3$		0.135	
$\alpha_O^g/\text{Å}^3$		0.465	
$\alpha_{\text{water}}^g/\text{Å}^3$			1.445 <sup>h</sup>
$D^h/10^{-9} \text{ m}^2 \text{ s}^{-1}$	2.5	$3.1 \pm 0.5$	2.7 (305 K)

<sup>a</sup> The internal geometry parameters of water are 1.0 Å and 109.5° for the distance and HOH angle, respectively. <sup>b</sup>  $A_{ij} = 4\epsilon\sigma^{12}$ ,  $C_{ij} = 4\epsilon\sigma^6$ ,  $\sigma$  and  $\epsilon$  are the Lennard-Jones parameters, and  $q_H$  and  $q_O$  are charges for the Coulombic part of the water model;  $T$  is the average temperature and  $P$  the target pressure during the simulations. <sup>c</sup> The average interaction energy of a water molecule in the liquid and (for POL1) the polarization component. <sup>d</sup> The density of liquid water. <sup>e</sup> The dimer energy and the distance are obtained after energy minimization. Experimental values in ref 15 for the dimer energy and O...O distance. <sup>f</sup> The total dipole  $\mu_{\text{tot}}$  is obtained from the sum of squared  $\mu_{\text{perm}}$  and  $\mu_{\text{induced}}$ . The diffusion coefficient is obtained from the slope of the mean-square displacement versus time. <sup>g</sup> Values for POL1 from ref 12. <sup>h</sup> Unless otherwise specified from ref 16.

at too short an O-O distance compared to the X-ray data.<sup>17</sup> The too short O-O distance likely occurs because of the simple form of the repulsion (proportional to  $r^{12}$ ),<sup>18</sup> but the shape of the curve is similar to the experimental one. The oxygen-hydrogen and hydrogen-hydrogen RDF's are presented in Figures 2 and 3. They agree very well with available computer simulations<sup>3,4</sup> and X-ray data.<sup>17</sup>

The permanent dipole in this model is 2.03 D, the induced dipole obtained with this model is 0.51 D, and the total average dipole moment of a water in liquid is  $\sim 2.52$  D (Table I). From the magnitude of these values, it is clear that the induced dipoles tend to be aligned in the same direction as the permanent moment. These results agreed quite well with the 2.6 D estimated by Coulson and Eisenberg<sup>19</sup> for the dipole moment of a water molecule in ice and in liquid water. It also is consistent with the calculation of Barnes et al.,<sup>6</sup> which led to a dipole moment of 2.5 D. The induced dipole moment of POL1 is 0.6 D smaller than that found by Ahlstrom et al.<sup>7</sup>

The permanent dipole moment of our model is somewhat larger than the gas-phase value because an atom-centered three-point-charges model cannot reproduce both the dipole and quadrupole moment of a water molecule.<sup>16</sup> For example, charges that reproduce the dipole moment lead to a quadrupole moment about 40% less than experiment. POL1 has a quadrupole moment about 30% less than experiment. We have shown the critical role of both the dipole and quadrupole moment in simulating hydrogen bond strengths and directionality of polar molecules.<sup>20</sup> Thus, our fixed charges are appropriate and reasonable monomer values.

It will be interesting to derive electrostatic potential based charges<sup>21</sup> by use of an ab initio wave function, with a large basis set and including correlation effects such that it reproduces the monomer dipole and quadrupole moments. Fitting the electrostatic

(14) Singh, U. C.; Weiner, P. K.; Caldwell, J.; Kollman, P. *Amber 3.0*; University of California: San Francisco, 1986.

(15) Odutola, J. A.; Dyke, T. R. *J. Chem. Phys.* **1900**, *72*, 5052 and references cited therein.

(16) Eisenberg, D.; Kauzmann, W. *The Structure and Properties of Water*; Oxford University Press: London, 1969.

(17) Soper, A. K.; Phillips, M. G. *Chem. Phys.* **1986**, *107*, 47.

(18) Reimers, J.; Watts, R.; Klein, M. *Chem. Phys.* **1982**, *82*, 95.

(19) Coulson, C. A.; Eisenberg, D. *Proc. R. Soc. London, A* **1966**, *291*, 445,454.

(20) Kollman, P. *Acc. Chem. Res.* **1977**, *10*, 365.

(21) Dzidic, I.; Kebarle, P. *J. Phys. Chem.* **1970**, *74*, 1466.

**Table II.** Energy Components (kcal/mol) for Ion-(H<sub>2</sub>O)<sub>n</sub> Complexes after Minimization

complex	$U_{\text{pair}}^a$	$U_{\text{pol}}^b$	$U_{3\text{-body}}^c$	$U_i$	expt <sup>e</sup>
Na <sup>+</sup> -(H <sub>2</sub> O) <sub>1</sub> <sup>f</sup>	-20.20	-3.77		-23.97	-24.00
Na <sup>+</sup> -(H <sub>2</sub> O) <sub>4</sub> <sup>g</sup>	-71.88	-6.99	4.86	-74.01	-74.10
Na <sup>+</sup> -(H <sub>2</sub> O) <sub>6</sub> <sup>h</sup>	-92.00	-12.20	5.59	-98.61	-96.40
Na <sup>+</sup> -(H <sub>2</sub> O) <sub>6</sub> (octa) <sup>i</sup>	-91.52	-7.19	10.02	-88.69	
Cl <sup>-</sup> -(H <sub>2</sub> O) <sub>1</sub> <sup>j</sup>	-10.80	-2.35		-13.15	-13.10
Cl <sup>-</sup> -(H <sub>2</sub> O) <sub>4</sub> <sup>k</sup>	-46.58	-10.46	8.95	-48.09	-48.60

<sup>a</sup> Portion of total complex formation energy from pairwise additive terms: for Na<sup>+</sup>,  $\sigma = 2.40 \text{ \AA}$ ,  $\epsilon = 0.13 \text{ kcal/mol}$ ; for Cl<sup>-</sup>,  $\sigma = 4.27 \text{ \AA}$ ,  $\epsilon = 0.25 \text{ kcal/mol}$ . <sup>b</sup> Portion of total complex formation energy from polarization term: for Na<sup>+</sup>,  $\alpha = 0.25 \text{ \AA}^3$ ; for Cl<sup>-</sup>,  $\alpha = 3.25 \text{ \AA}^3$ . <sup>c</sup> Portion of total complex formation energy from three-body-exchange repulsion term: for Na<sup>+</sup>,  $A = 8.5 \times 10^6 \text{ kcal/mol}$ ;  $\beta = 3.35 \text{ \AA}^{-1}$ ;  $\gamma = 0.10 \text{ \AA}^{-1}$ ; for Cl<sup>-</sup>,  $A = 7500 \text{ kcal/mol}$ ;  $\beta = 1.18 \text{ \AA}^{-1}$ ,  $\gamma = 0.35 \text{ \AA}^{-1}$ . <sup>d</sup> Total energy of complexation. <sup>e</sup> Reference 21. <sup>f</sup> Optimized Na<sup>+</sup>-(H<sub>2</sub>O)<sub>1</sub> structure,  $R(\text{Na}^+\text{-O}) = 2.24 \text{ \AA}$ . <sup>g</sup> Tetrahedral cage of water molecules around ion,  $R(\text{Na}^+\text{-O}) = 2.35 \text{ \AA}$ . <sup>h</sup> Structure with 4 + 2 geometry (see ref 10). <sup>i</sup> Octahedral coordination around ion,  $R(\text{Na}^+\text{-O}) = 2.40 \text{ \AA}$ . <sup>j</sup> Optimized Cl<sup>-</sup>-(H<sub>2</sub>O)<sub>1</sub> structure,  $R(\text{Cl}^-\text{-O}) = 3.30 \text{ \AA}$ . <sup>k</sup> Optimized Cl<sup>-</sup>-(H<sub>2</sub>O)<sub>4</sub> structure (see ref 10).

potential derived charges to a four-point model should allow reproduction of both dipole and quadrupole moments. On the other hand, fitting the charges to a three-point atom-centered model will require a compromise, so that the dipole and quadrupole moments cannot both be reproduced.

To support the above assumption, we have also carried out preliminary simulations on a nonadditive four-point water model with a charge distribution similar to the one presented in ref 18. That model accurately represents both gas-phase dipole and quadrupole moments. It appears to be a slight improvement over the one presented here, with an increase in depth of the minimum in the O-O radial distribution function at  $\sim 3.5 \text{ \AA}$ .

We have also carried out calculations on ion-water clusters of Na<sup>+</sup>(H<sub>2</sub>O)<sub>n</sub> and Cl<sup>-</sup>(H<sub>2</sub>O)<sub>n</sub> with  $n = 1-6$ . The ion van der Waals parameters were derived by requiring the ion-(H<sub>2</sub>O)<sub>1</sub> complex to fit the ab initio calculated distance and experimental enthalpy of complex formation. Then, the three-body exchange repulsion was calibrated on experimental and ab initio data for ion-(H<sub>2</sub>O)<sub>2</sub> clusters. We closely followed the approach of ref 10 in this parameterization. The derived parameters (Table II) are not unique, but a reasonable set. The results are summarized in Table II. They are in excellent agreement with experiment<sup>22</sup> and with the earlier simulations of Lybrand et al.<sup>10</sup>

We have explored the use of both POL and POL1 in these ion-water simulations. The latter model has led to better behavior not only on liquid water (discussed previously) but also in the studies of ion-water clusters. It led to a Na<sup>+</sup>-H<sub>2</sub>O distance and energy, with use of a unit charge on Na<sup>+</sup>, in good agreement with experiment, whereas the model with the entire molecular polarizability on the oxygen ( $\alpha = 1.44 \text{ \AA}^3$ ) led to a Na<sup>+</sup>-H<sub>2</sub>O energy 6 kcal/mol too exothermic at the Na<sup>+</sup>...O distance of 2.24 Å. Thus, the same distributed polarizability model (POL1) appears to be a good choice for the liquid and ionic solutions.

## Discussion

Let us compare our model with other explicit nonadditive water models presented recently. It is most similar to that of Ahlstrom

et al.<sup>7</sup> in its use of atom-centered inducible point dipoles, but our use of atom-centered polarizabilities rather than the molecular value appears to be an improvement, particularly in the representation of ion-water interactions.

Sprink and Klein<sup>8</sup> have presented an interesting model, in which nonadditive effects have been included by allowing the partial charges to move. This approach would be harder to generalize to more complex molecules than H<sub>2</sub>O, but has the advantage that one need not include analytical derivatives of the dipole-dipole energies in the molecular dynamics algorithm. Nonetheless, the model that they present<sup>8</sup> does not appear to reproduce the water liquid properties as well as POL1.

Clementi and co-workers<sup>1</sup> have presented two nonadditive models, in which counterpoise corrections are either neglected or included. These are much more complicated than POL1, since they are derived to fit quantum mechanical energy surfaces. They do not fit the water liquid properties as well as POL1. The use of bond rather than atomic polarizabilities in ref 1 is another difference with POL1. Placing the polarizabilities on the bonds is reasonable but adds to the numbers of centers that must be considered.

We have not included the vibrational quantum correction, estimated by Kuharsky and Rossky<sup>23</sup> as  $\sim 0.8 \text{ kcal/mol}$ , mainly because this correction would not be easy to generalize to other more complex molecules. In addition, we have neglected charge transfer and other more complex intermolecular interaction energies. We have not evaluated the heat capacity and dielectric constant for our model; however, it is encouraging that the SPC/E model leads to good agreement with experiment for these two properties. We are currently working on methods to make the algorithm more efficient using predictor-corrector approaches<sup>7</sup>, which should facilitate the evaluation of heat capacity, dielectric constant, and other fluctuational properties, which require much longer simulations. We are also exploring the use of four-point models and models that allow internal flexibility.

But already at this point our approach seems to be currently among the most reasonable, effective, and useful approaches to the inclusion of nonadditive effects in condensed-phase simulations of water and aqueous solutions. The use of atom-centered polarizabilities has the added benefit that the software is in place to include permanent-point dipoles in general molecular mechanical models to improve the electrostatic representation of more complex molecules.

## Conclusion

We have constructed a polarizable water model using molecular dynamics techniques. The calculated structural and thermodynamic properties presented here are good, but not perfect. However, at this point the flaws are of quantitative nature. We feel we have taken a significant step forward in our ability to simulate molecular interactions with ever increasing accuracy using empirical energy functions.

**Acknowledgment.** We acknowledge support of the NSF (CHE-85-10066) to P.A.K., the Macromolecular Workbench (ONR-N00014-86-K-0757, R. Langridge, PI), and the San Diego Supercomputer Center. L.X.D. thanks D. Mclean, J. Rice, and B. Liu for their encouragement in pursuing this project. The calculations were carried out on the IBM 3090 at the Almaden Research Center, IBM Research Division.

(22) Singh, U. C.; Kollman, P. J. *Comput. Chem.* **1984**, *5*, 129.

(23) Kuharsky, P.; Rossky, P. A. *J. Chem. Phys.* **1985**, *82*, 7734.